

CHARACTERIZATION OF STRING RIBBON SILICON MATERIAL AND SOLAR CELLS

P. Geiger, G. Hahn, P. Fath, E. Bucher, R. Wallace*

Universität Konstanz, Fachbereich Physik, Fach X916, 78457 Konstanz, Germany

Tel.: +49-7531-88-2132, Fax: +49-7531-88-3895, e-mail: patric.geiger@uni-konstanz.de

*Evergreen Solar Inc., 211 Second Ave., Waltham, MA 02154 USA

ABSTRACT: String Ribbon silicon, as supplied by Evergreen Solar Inc., is a promising cost effective alternative to standard cast multicrystalline silicon. The material properties of this ribbon silicon have been studied with respect to the optimization of solar cell processing.

The majority charge carrier transport has been investigated using temperature dependent Hall measurements. The results show a pronounced influence of hydrogen passivation on the Hall mobility at low temperatures. Furthermore, lifetime mappings have been performed which visualize strong variations in recombination activity throughout one wafer. In order to enhance the diffusion length, especially in areas of higher recombination, impurities have been removed by Al-gettering and P-Al-cogettering. For the same reason hydrogen passivation has been performed at different stages during solar cell processing using a remote hydrogen plasma. In this way it was possible to investigate the deleterious influence of the hydrogen treatment on the front grid and the space charge region as well as hydrogen effusion during following thermal processing steps.

Keywords: Ribbons – 1: Characterisation – 2: Passivation – 3

1. INTRODUCTION

Material losses due to dicing of silicon ingots should be avoided in order to reduce the cost of multicrystalline (mc) silicon for solar cell applications. String Ribbon wafers are pulled out of the melt in the required thickness and are therefore a promising alternative to mc silicon cut out of ingots [1]. As ribbons usually contain more crystal defects than standard cast mc silicon the minority charge carriers show a lower diffusion length within String Ribbon. Consequently, it is necessary to study the specific material properties and exploit the results for optimizing the solar cell process.

2. HALL MEASUREMENTS

Temperature dependent Hall measurements have been performed in order to study the electrical material properties of String Ribbon silicon. In addition to the usual preparation of the samples by defect etching and contact formation [2], some of the samples were levelled with a commercial dicing saw and/or passivated in a Microwave Induced Remote Hydrogen Plasma (MIRHP) passivation system. Unfortunately it was not feasible to measure the same sample before and after hydrogen treatment because of contamination problems. Therefore we were restricted to the comparison of specimens originating from the same wafer.

Nevertheless, Fig. 1 shows clearly a passivating effect of the MIRHP on the String Ribbon material: At temperatures below 300 K the mobilities $\mu_H(T)$ of the samples #2 and #3 are much higher than of the unpassivated one #1. However, a beneficial influence of the hydrogen treatment on processed solar cells can also be seen at room temperature as will be shown later. This might be an indication for “sleeping” defects, which are not active at temperatures above 200 K, but which are activated by thermal treatments necessary for the processing of solar cells [3]. Temperature dependent Hall measurements reveal these defects because the corresponding defect states are charged with increasing

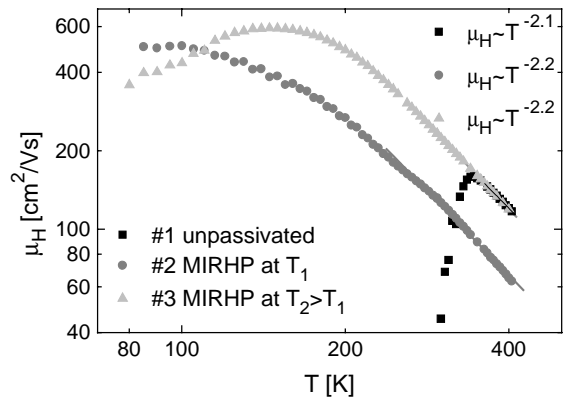


Figure 1: Influence of MIRHP passivation on the Hall mobility $\mu_H(T)$ of different String Ribbon samples with levelled front sides: Not passivated (#1), MIRHP passivated at temperature T_1 (#2), MIRHP passivated at temperature $T_2 > T_1$ (#3). At $T > 150$ K the different mobilities of samples #2 and #3 are due to variations in the material quality.

temperature according to a rising Fermi energy level. In this case the band bending caused by the charged defect states impedes the movement of majority charge carriers (holes) and therefore reduce their mobility. As the temperature further increases the influence of the defect states diminishes due to a higher kinetic energy of the charge carriers. At room temperature this energy is high enough that an influence of the defect states on the mobility is no longer visible. This leads to the minimum in the mobility curve of sample #4 in Fig. 2 [4].

By fitting the charge carrier mobilities at high temperatures the exponents given in Fig. 1 have been obtained which agree very well with the experimentally determined value of 2.2 for holes in monocrystalline silicon [5].

Furthermore, Hall measurements have been performed on samples with different surface treatments, i.e. no, one or both sides levelled. The mobilities given in Fig. 2 as well

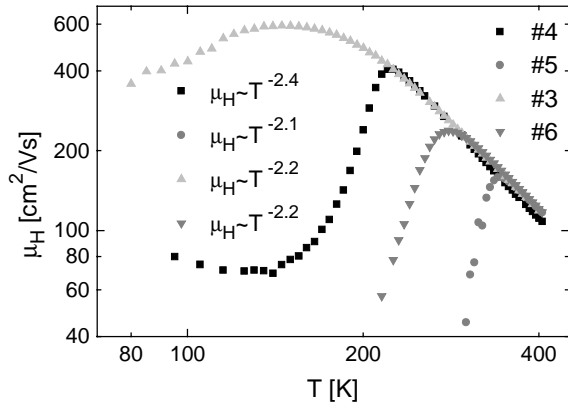


Figure 2: Hall mobility $\mu_H(T)$ of samples with different surface treatments: Not levelled (#4), front side levelled (#5), front side levelled and MIRHP passivated (#3), both sides levelled (#6).

as the investigated conductivity or majority charge carrier density do not show a clear dependence on the surface treatment. Consequently the quality variation within the wafer seems to have at least as much influence on the mentioned parameters as the surface levelling.

3. LIFETIME MAPPING

3.1 Surface passivation

For the determination of the minority carrier lifetime τ a commercial microwave detected photoconductivity decay (PCD) measurement system was used. With this method an effective lifetime τ_{eff} is measured which includes the bulk lifetime τ_b and the recombination at the wafer surface via:

$$\frac{1}{\tau_{eff}} = \frac{1}{\tau_b} + \frac{1}{\tau_{surface}}$$

In order to passivate the surface and detect τ_b a HF-dip was performed before the first measurement was started under bias light. In the following several mappings (step-width 1 mm) of the same wafer have been performed under low injection conditions, which demonstrates the gradually

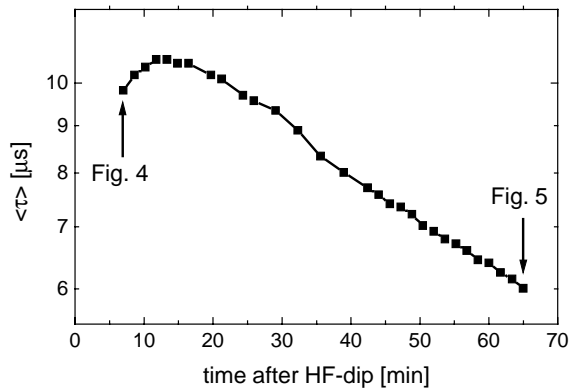


Figure 3: Mean lifetime in dependence on time passed since HF-dip. The mappings displayed in Figs. 3 and 4 are marked with arrows.

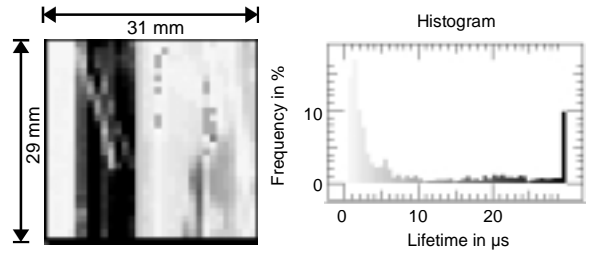


Figure 4: Lifetime mapping and corresponding histogram of a selected area of a String Ribbon wafer 7 minutes after the HF-dip.

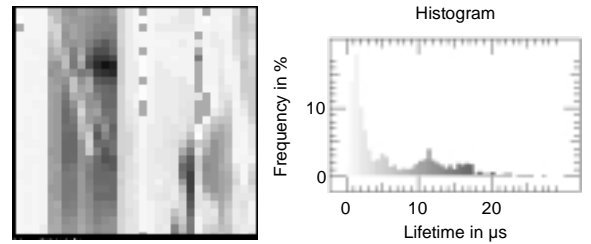


Figure 5: Lifetime mapping of the same area as in Fig. 4 and corresponding histogram 65 minutes after HF-dip.

increasing influence of the surface recombination due to a vanishing HF passivation (Fig. 3). Two of the obtained mappings are shown in Figs. 4 and 5. In all these pictures a stripe-like structure, which is aligned with the growth direction of the ribbon and reflects the grown-in crystallography, as well as strong variations in lifetime are evident. Usually multiple successive lifetime measurements are performed in order to have the possibility of extrapolating the curve shown in Fig. 3 so that a value for the initial bulk lifetime of the minority charge carriers is obtained. Paradoxically $\tau(t)$ increases during the first 12 minutes instead of starting to decrease instantaneously after the HF-dip. Consequently it is rather difficult to determine the bulk lifetime of the wafer. This effect might be related to another difficulty that occurs when measuring lifetimes in String Ribbon wafers.

3.2 Variations in recombination activity

The PCD technique requires the choice of an adequate time range within which the transient recorder evaluates the PCD. Due to the strongly varying recombination activity a well suited time range can only be chosen for small homogeneous wafer areas. Measurements of the whole wafer or large areas result in graphs given in Fig. 6. If a wide time range is chosen areas of low lifetime cannot be measured properly and are either neglected by the computer software during the calculation of the mean lifetime or taken into account with wrong values. Vice versa a small time range is not adequate for areas of higher lifetime. As a consequence it is only possible to get an impression of the distribution of points of high and low lifetime within a wafer or selected areas but not to obtain reliable mean lifetimes for a whole wafer or square centimetre sized regions. For the same reason the determination of the mean bulk lifetime of larger wafer areas by extrapolation as suggested by the dashed line in Fig. 6 is not reliable.

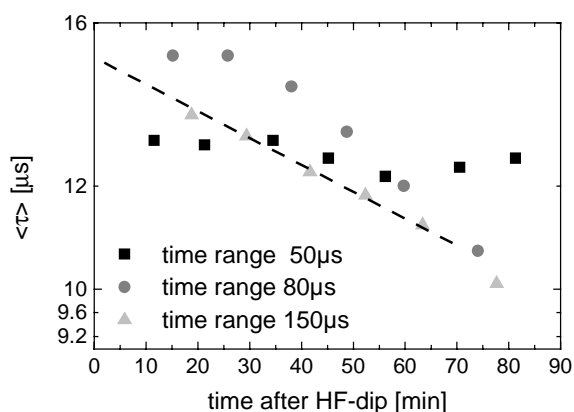


Figure 6: Mean lifetime measured at the same wafer area using different time ranges for the transient recorder of the PCD system.

Furthermore, the increase of lifetime during the first 12 minutes in Fig. 3 might also be attributed to a non adequate time range of the transient recorder so that very high lifetimes could not be taken into account during the calculation of the mean lifetime. As similar effects occurred sometimes less distinctively also on monocrystalline silicon which allows a more precise choice of the time range, further measurements have to be performed in order to find out for certain about the reason for this behaviour.

4. STRING RIBBON SOLAR CELLS

It has been shown in [6] that improvements of solar cells made from different mc materials can be achieved by Al-gettering and MIRHP passivation. As String Ribbon wafers were not included in this study we have investigated the prementioned processing steps implemented in the processing sequence given in Fig. 7.

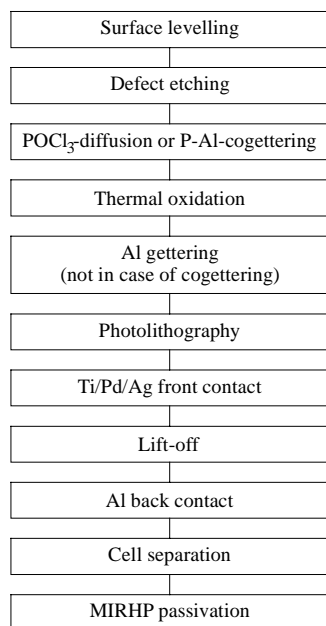


Figure 7: Schematic overview of the process sequences.

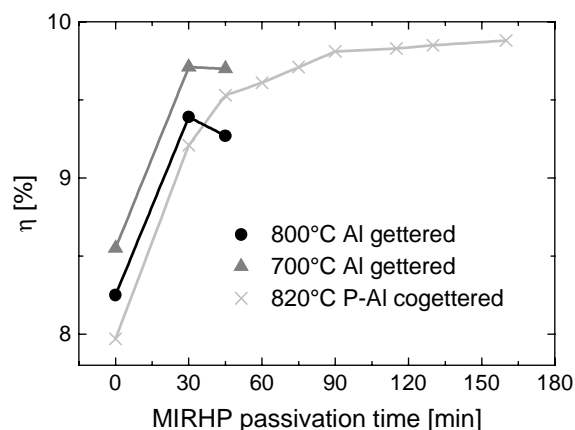


Figure 8: Efficiency η of solar cells gettered in different ways after various passivation times.

Resulting efficiencies η of solar cells with an area of $2 \times 2 \text{ cm}^2$ are shown in Fig. 8. When analyzing the data one should keep in mind the strong variations in material quality. Because differences in cell parameters could also be due to these variations it is difficult to compare the solar cells Al-gettered at different temperatures. However, as the efficiencies of P-Al-cogettered solar cells have been lower than those of the Al-gettered counterparts in all investigations it is quite sure that this can be blamed on the different gettering steps. Furthermore, it could be observed that it takes longer to passivate a P-Al-cogettered solar cell than a Al-gettered one. But during the MIRHP-passivation the cogettered cells gradually catch up with the Al-gettered cells. In this way increases in V_{OC} of up to 30 mV, in J_{SC} of up to 2.6 mA/cm^2 and in FF up to 2.2% absolute have been reached. Final cell parameters of selected String Ribbon solar cells are given in Table I together with those of Bayer BaysixTM mc Si cells which have been processed simultaneously for monitoring reasons. Although the P-Al-cogettered String Ribbon solar cell shows a higher efficiency than the Al-gettered one this cannot be considered as a general fact because of the influence of the varying material quality.

	String Ribbon		Baysix TM -mc	
	Al	P-Al	Al	P-Al
V_{OC} [mV]	568	571	596	598
J_{SC} [mA/cm ²]	22.1	22.7	22.5	22.7
FF [%]	77.3	76.2	78.4	77.0
η [%]	9.7	9.9	10.5	10.5
R (905 nm) [%]	32	32	32	33

Table I: Parameters of selected String Ribbon cells and simultaneously processed Bayer BaysixTM monitor cells (without any antireflection coating, R reflectivity).

It might happen that front contact metal diffuses into the space charge region during the thermal treatment in the MIRHP passivation step and causes a degradation of the fill factor. As this effect as well as the effusion of the hydrogen out of the solar cells depends strongly on the temperature an optimized passivation temperature has to be found. A possible way to avoid the problem of metal penetrating into the space charge region is to passivate the

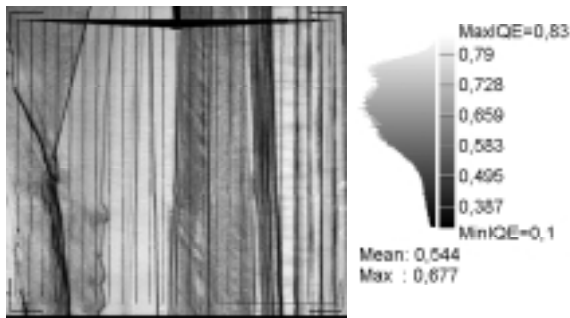


Figure 9: LBIC IQE mapping of a String Ribbon Solar Cell before hydrogen passivation and corresponding histogram (resolution 30 μm).

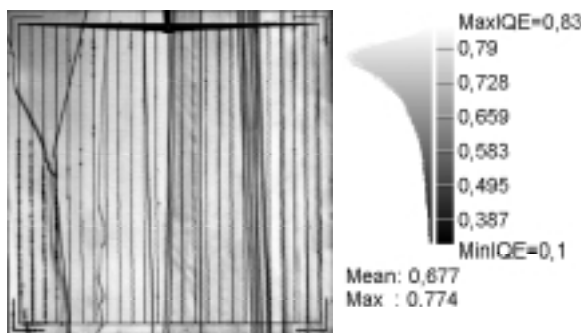


Figure 10: IQE mapping and corresponding histogram of the same solar cell as in Fig. 8 after 30 minutes of MIRHP passivation (laser wavelength 905 nm, resolution 30 μm).

wafers with hydrogen before metallization. Therefore, we exposed some wafers to the MIRHP for three hours and performed photolithography afterwards. After contact formation the solar cells were measured and MIRHP passivated again. In most cases we found a further improvement of the cell parameters after the second MIRHP step. Most probably this is due to effusion of hydrogen originating from the first MIRHP step before metallization during the last contact annealing step.

In order to get further information about the influence of the hydrogen passivation on String Ribbon material, the Internal Quantum Efficiency (IQE) has been mapped after various passivation steps using a Laser Beam Induced Current (LBIC) system and a laser wavelength of 905 nm (penetration depth ca. 30 μm). Fig. 9 shows the IQE mapping of an Al-gettered solar cell before hydrogen treatment. Areas of quite good IQE are visible as well as regions of relatively low performance. On the whole they lead again to a stripe-like pattern of the mapping and a widely distributed histogram. After 30 minutes of MIRHP passivation the same cell was mapped again. In the resulting picture given in Fig. 10 the stripe-like structure is no longer visible as clearly as in Fig. 9. An increase in the IQE has been achieved in nearly all parts of the cell. Particularly areas with a formerly quite low performance show large improvements in the IQE, whereas the very best areas in Fig. 9 have improved less. This leads to a more homogeneous solar cell, as illustrated by the narrowing of the distribution in the histogram of Fig. 10. Nevertheless, there are also a few narrow areas adjacent to grain boundaries which seem to be nearly unpassivable. This could be due to

precipitates causing shunt like mechanisms in the space charge region.

SUMMARY

String Ribbon silicon is a promising material for cost effective solar cell production. Its electrical transport properties are strongly enhanced by hydrogen passivation whereas the surface treatment is less influential. The accurate determination of the mean bulk lifetime on wafer areas in the square centimetre range or on whole wafers using the PCD technique is problematic. It is not possible to select an adequate time range for the transient recorder according to the strongly varying lifetimes within the selected wafer area. Lifetime mappings, however, reveal areas of lower and higher recombination rates which show a stripe like structure aligned with the growth direction of the ribbon. The enhancement of the diffusion length during cell processing can be done by Al- or P-Al-cogettering steps and hydrogen passivation. It has been shown that the gettering and the passivation parameters have to be matched with each other in order to achieve high efficiencies. As it is not possible to passivate bulk defects durably before metallization, it is particularly necessary to optimize MIRHP passivation parameters and in this way prevent or minimize penetration of metal into the space charge region as well as damage of the surface by the hydrogen plasma.

ACKNOWLEDGEMENTS

We like to thank M. Keil and B. Fischer for technical assistance during cell processing and characterization.

REFERENCES

- [1] R. L. Wallace, J. I. Hanoka, S. Kamra, A. Rohatgi, Proc. 14th EC PVSEC, Barcelona (1997) 171.
- [2] L. J. van der Pauw, Philips Res. Repts. **13** (1958) 1-9.
- [3] I. Perichaud, S. Martinuzzi, Proc. 2nd WC PVSEC, Vienna (1998) 1290.
- [4] H. Nussbaumer, F. P. Baumgartner, G. Willeke, E. Bucher, J. Appl. Phys. **83** (1) (1998) 292.
- [5] H. J. Möller, Semiconductors for Solar Cells, Artech House, London, ISBN 0-89006-574-8.
- [6] G. Hahn, W. Jooß, M. Spiegel, P. Fath, G. Willeke, E. Bucher, Proc. 26th IEEE PVSC, Anaheim (1997) 75.